Bulletin of the
Seismological Society of America

Vol. 81 December 1991 No. 6

ESTIMATION OF GROUND MOTION AT DEEP-SOIL SITES IN EASTERN NORTH AMERICA

By David M. Boore and William B. Joyner

Abstract

The stochastic model used previously to estimate motions at hard-rock sites in eastern North America has been modified to include the effect of deep soils. We simulated motions for a number of distances and magnitudes for a representative soil column and used these motions to derive equations giving ground motion as a simple function of magnitude and distance. These new equations are intended for use in building codes and those engineering applications that do not require detailed site evaluations. The ground motions for which we derived equations include 5%-damped response spectra at 13 periods ranging from 0.05 to 4 sec, peak acceleration and the maximum pseudovelocity and maximum pseudoacceleration responses. The latter two quantities are introduced here for the first time. They represent the maxima over the period range 0.1 to 4 sec for a given magnitude and distance, and they may be useful as a basis for determining the seismic coefficient in building codes.

Introduction

Equations giving ground motion as a function of magnitude and distance were published by Boore and Atkinson (1987) for hard-rock sites in eastern North America. These equations were obtained by fitting a parametric model to synthetic ground motions computed from the stochastic model introduced by Hanks and McGuire (1981; see Joyner and Boore, 1988, for a recent summary of the method). The equations are for distances less than 100 km and are relatively complex. Recognizing the need for estimation of motions at greater distances and the desirability of a simpler functional form, particularly in probabilistic hazard analyses, Atkinson and Boore (1990) published new equations valid for distances up to 400 km. With a minor exception (resulting from different choices of the geometrical spreading and Q functions for distances beyond about 100 km), the synthetic data to which the new equations were fit were the same as those used in Boore and Atkinson (1987). In this paper, we continue the evolutionary sequence by presenting equations for ground motions on generic deep-soil sites ("S2" soil conditions in the terminology of recent editions of the Uniform Building Code or the Building Seismic Safety Council Provisions). The equations give peak acceleration, response spectral values, and two newly defined quantities proposed as an alternative basis for building codes. These new equations are intended for use in building codes and those engineering applications that do not require detailed site evaluations. They are applicable over broad areas and are not intended for site-specific evaluations of ground motion.

Method

The essential difference between this paper and the papers of Boore and Atkinson (1987) and Atkinson and Boore (1990) is that the effect of a soil column is included here. A frequency-domain filter is derived that approximates the amplification and attenuation of the soil column. This filter is used along with a specified source-scaling relation in the simulation of ground motions for a set of distances and magnitudes. Because the magnitude and distance dependence of the ground motions is a complicated function of a number of parameters and equations, it is not practical to derive an expression for this dependence directly from the underlying equations. Instead, the simulated motions are treated as if they were an observed data set; an attenuation equation is fit to the simulated ground motions, in the same way that empirical attenuation equations are derived from observed data. The coefficients in the attenuation equation are determined using the two-stage regression introduced by Joyner and Boore (1981).

The effect of the soil column is approximated by the method suggested by Joyner *et al.* (1981). The procedure is based on the nonresonant amplification produced as a result of energy conservation of waves propagating through materials of gradually changing velocity. For high frequencies, this amplification is given by

$$A = \sqrt{\rho_0 \beta_0 / \rho_s \beta_s}, \tag{1}$$

where ρ and β are the density and shear velocity and the subscripts indicate the properties at the earthquake source (subscript 0) and at the site (subscript s). In general, there is much less variation in density than in shear velocity, and variation in density will be ignored in this study. Joyner *et al.* (1981) introduced frequency dependence for the amplification given in equation (1) by substituting a frequency-dependent effective velocity for β_s. They defined the effective velocity at a particular frequency as the average velocity from the surface to a depth of a quarter wavelength. Specifically, the depth is found from which the accumulated travel time to the surface is one quarter of a given period, and that depth is divided by the accumulated travel time to yield an average velocity for the period. Substituting this effective velocity into equation (1) produces a frequency-dependent amplification.

The soils will also produce attenuation, particularly at high frequencies, and these are accounted for by the equation

$$P(f) = \exp(-\pi \kappa_0 f), \tag{2}$$

where κ_0 is obtained by integrating $z/(\beta Q)$ over the thickness of the soil column (where z is depth and β and Q are the shear velocity and a frequency-independent measure of damping, respectively, at that depth). In Appendix A, we test the approximations embodied in equations (1) and (2) by comparing the results with those from a calculation that accounts for the wave propagation in a soil column.

The Soil Column and Its Effects

Our approach is to derive the ground motions for a single soil profile whose properties represent an average of the properties of many individual profiles. This differs from Bernreuter *et al.* (1985), who use a Monte Carlo scheme in

which motions are computed for a series of soil columns obtained from perturbations of an average profile. Unlike our method, their scheme can provide estimates of the uncertainty in the predicted motion, estimates whose validity depend on the accuracy of the distribution function of the material properties. Our approach, however, is much less computer intensive and should provide a reasonable approximation to the median ground motions.

In this study, we restrict our attention to sites underlain by deep soils (the S2 category in the 1988 Building Seismic Safety Council (BSSC) Provisions or the 1988 Uniform Building Code (UBC), defined in the UBC as "a soil profile with dense or stiff soil conditions, where the soil depth exceeds 200 feet [60 m]"). The ground-motion equations must be applicable in a broad sense to total soil depths from the 60-m minimum that defines S2 to many hundreds of meters. The counteracting effects of attenuation and amplification will produce depth-dependent soil response: short-period response will be higher for shallow deposits because the attenuation represented by κ_0 is less; longer-period response will be higher for deep deposits because the low-frequency β_s is smaller (this is illustrated later in Fig. 3). We do not want the equations to underestimate the response to a significant degree for any common site conditions that fit the definition of S2. To accomplish that purpose, we were forced to use a soil column that does not represent any real site or even the average of a number of real sites: the attenuation was computed over a smaller-than-average depth range, and the thickness is greater than usual. In addition, the density is constant.

The shear velocities in the upper part of the soil column were based on Bernreuter *et al.*'s (1985) compilations from a number of deep soil sites (Fig. 1). We used the average shown by the dark line in the figure to a depth of 150 m. Below this, we included a thick portion of constant velocity in the lower portion

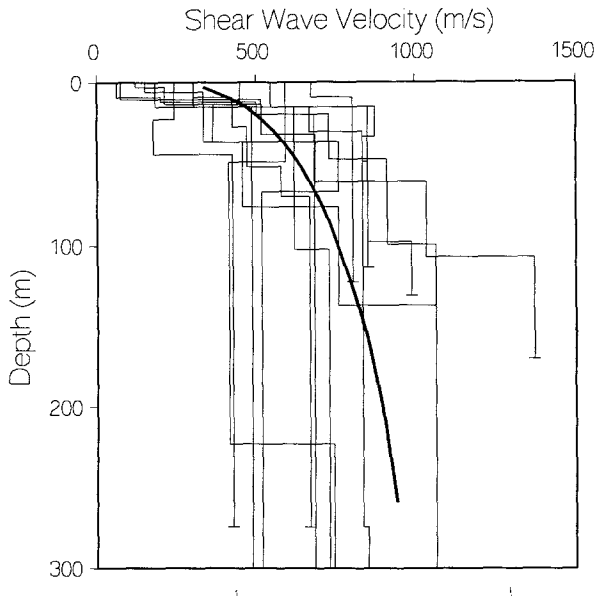

FIG. 1. Shear velocity as a function of depth for an average deep-soil site (heavy line), based on a compilation of velocities from PSAR and FSAR reports for nuclear power-plant sites throughout the United States (light lines). The short horizontal bars indicate bedrock. (Adapted from a figure in Bernreuter *et al.*, 1985.)

of the soil column, before terminating the column with a hard-rock half-space. The total thickness of the column was taken as 650 m, consistent with the depth of the sediments in the Mississippi embayment (Andrews and Mooney, 1985). This is probably thicker than most deep-soil sections in eastern North America, but the greater-than-average depth leads to conservative estimates of the soil response at low frequencies.

For the attenuation we assigned Q values to the layers that are reasonably consistent with those inferred by Andrews in the Mississippi embayment (M. Andrews, written comm., 1990). The κ_0 used in the ground-motion simulations (0.02) was based on the value corresponding to the upper 100 m of the soil section, with a small allowance for attenuation in the rock below (this additional κ_0 corresponds to an f_{max} of about 40). This has the effect of producing less attenuation than would probably occur for a soil column as thick as 650 m.

The parameters of the generic deep-soil column that we used to derive the amplification and attenuation are tabulated in Table 1 and plotted in Figure 2. Also included in the table are columns giving four times the cumulative travel time and the cumulative κ_0 from the surface down. These columns are useful in assessing the relative contributions of various parts of the soil section to the amplification and attenuation of the waves.

TABLE 1

MATERIAL PROPERTIES FOR A DEEP-SOIL SITE

Layer	Depth to Top (m)	Thickness (m)	Shear Velocity (m/sec)	Q	Density (gm/cm^3)	4 × Cum. Time (sec)	Cum. κ_0 (sec)
1	0.0	0.9	285	10	2.0	0.00	0.000
2	0.9	1.7	320	10	2.0	0.01	0.000
3	2.6	3.2	384	10	2.0	0.03	0.001
4	5.8	2.9	427	10	2.0	0.07	0.002
5	8.7	3.8	463	10	2.0	0.09	0.002
6	12.5	4.4	500	10	2.0	0.13	0.003
7	16.9	4.1	524	10	2.0	0.16	0.004
8	21.0	4.9	555	10	2.0	0.19	0.005
9	25.9	4.6	570	10	2.0	0.23	0.006
10	30.5	4.9	590	10	2.0	0.26	0.007
11	35.4	5.8	607	10	2.0	0.29	0.007
12	41.1	5.2	628	10	2.0	0.33	0.008
13	46.3	5.5	643	10	2.0	0.37	0.009
14	51.8	5.2	661	10	2.0	0.40	0.010
15	57.0	5.5	674	10	2.0	0.43	0.011
16	62.5	6.1	689	10	2.0	0.46	0.012
17	68.6	6.1	707	10	2.0	0.50	0.012
18	74.7	6.1	719	10	2.0	0.53	0.013
19	80.8	6.1	732	20	2.0	0.57	0.014
20	86.9	6.1	744	20	2.0	0.60	0.015
21	93.0	7.0	759	20	2.0	0.63	0.015
22	100.0	6.1	771	20	2.0	0.67	0.015
23	106.1	6.7	783	20	2.0	0.70	0.016
24	112.8	6.7	792	20	2.0	0.74	0.016
25	119.5	6.6	808	20	2.0	0.77	0.017
26	126.0	7.2	820	20	2.0	0.80	0.017
27	133.2	7.0	832	50	2.0	0.84	0.018
28	140.2	7.0	838	50	2.0	0.87	0.018
29	147.2	502.9	853	50	2.0	0.90	0.018
30	650.1	Half-space	3500	9999	2.0	3.26	0.030

The amplification was computed for a number of frequencies, using the effective velocity and equation (1). For use in computer programs, it is convenient to give the amplification as a continuous function of frequency. We approximated the response by a sequence of line segments; the equation for segment i is given by

$$\log A(f) = \log A_i + S_i \log f, \tag{3}$$

where the coefficients $\log A_i$ and S_i and the frequency range defining each segment are given in Table 2. The amplification and the combined effect of the amplification and the attenuation for the adopted model are shown in Figure 3. As frequency increases, there is little effect until a frequency of about 0.2 Hz is reached, at which point there is a rapid rise in the amplification to a factor greater than 2. (From Table 1 it can be seen that the sharp rise in amplification occurs for a period close to four times the cumulative travel time through the whole soil section—3.3 sec.) Without attenuation (plus signs in Fig. 3), the site response rises slowly with frequency; with attenuation, however, the response is almost constant up to a frequency of about 4 Hz. The attenuation factor reduces the combined effect to unity near 20 Hz, with a diminution at higher frequencies.

Also shown in Figure 3 are the soil-response filters for the generic model using the whole soil column (650 m) and the upper 60 m of the soil column. We assume that these two models are representative of the range of depths for S2 conditions. Unlike the adopted model used in the calculation of motions from

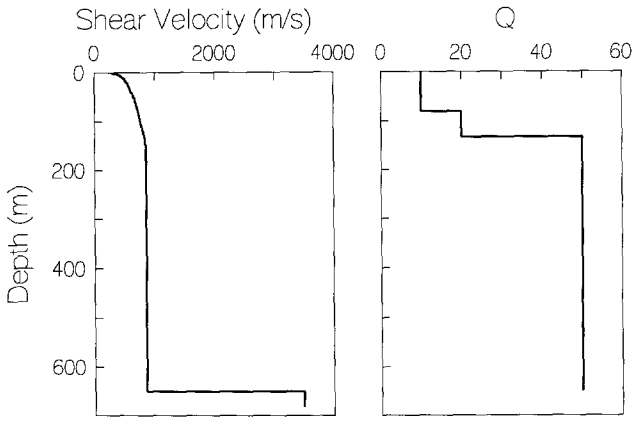

FIG. 2. Shear velocity and attenuation (Q) used in this paper for deep-soil sites.

TABLE 2

COEFFICIENTS FOR SHEAR-WAVE AMPLIFICATION FILTER

Segment	Frequency Range (Hz)	$\log A_i$	S_i
1	$f \leqq 0.01$	0.01	0.0
2	$0.01 \leqq f \leqq 0.11$	0.15	0.07
3	$0.11 \leqq f \leqq 0.20$	0.38	0.32
4	$0.20 \leqq f \leqq 0.35$	0.64	0.69
5	$0.35 \leqq f \leqq 20.0$	0.38	0.11
6	$20.0 \leqq f$	0.53	0.0

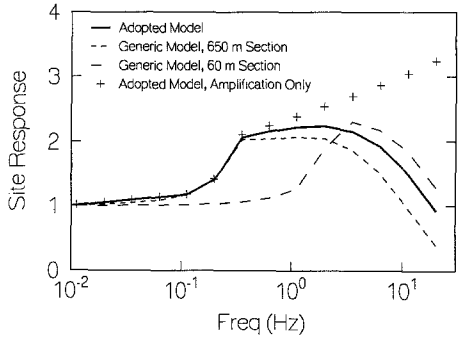

FIG. 3. The site-response filter for the adopted model (heavy line). For comparison, the site responses for models with thick and thin soil sections overlying bedrock are also shown (light lines), as is the response for the adopted model with no attenuation (this is the same amplification that would occur for the model with a 650-m soil section). The filter shown by the heavy line is used in the stochastic model to account for the response of deep-soil sites.

which the new attenuation equations were derived, the κ_0 for these models corresponds to the attenuation over the indicated depth (60 and 650 m), again with a small allowance for near-surface attenuation in the rocks below the sediments. The curves in Figure 3 illustrate the points made earlier about the hybrid nature of the adopted model: the model combines the amplification at low frequencies of the thick model and the attenuation at high frequencies of the thin model. (The soil-response filter for the adopted model does not envelope the other two responses because we used a somewhat larger κ_0 (0.02) than the value calculated for the thin model (0.015); κ_0 is not well determined, and our choice was guided but not constrained by the value for the thin model.)

SYNTHETIC GROUND MOTIONS

The next step in the analysis is to generate simulated ground motions for a set of magnitudes and distances. We did this using the stochastic model described elsewhere (e.g., Joyner and Boore, 1988), closely following Boore and Atkinson (1987) with Atkinson and Boore's (1990) choice of geometrical spreading and attenuation. The primary new feature in our analysis is to include the soil response given by equations (2) and (3). We also used a slight modification of Joyner's (1984) spectral model rather than the simple ω^{-2} source model used in the Boore and Atkinson papers. We did this because of the possible application of our results to the estimation of ground motions for very large earthquakes. We consider it likely that the source scaling changes for earthquakes larger than a critical size (such an earthquake, for example, might correspond to rupture through the brittle layer of the lithosphere), and it is awkward to account for this using the usual ω^{-2} model, which has only one corner frequency. Joyner's (1984) model, on the other hand, has two source corners, and he argues that the effect of the change in scaling can be included by fixing the higher-frequency corner at the value for the critical-sized earthquake.

The slight modification that we made to Joyner's model eliminates a kink in the spectral shape at the low-frequency corner. The source displacement spectrum is given by

$$S(f) = M_0 S_a S_b, \tag{4}$$

where M_0 is the seismic moment and

$$S_a = 1.0/\left(1.0 + \left(f/f_a\right)^2\right)^{0.75} \tag{5}$$

and

$$S_b = 1.0/\left(1.0 + \left(f/f_b\right)^2\right)^{0.25}. \tag{6}$$

The two corner frequencies, f_a and f_b, are given by equation (24) in Joyner and Boore (1988). The parameters controlling the values of the corner frequencies are β_0 (shear velocity near the source), λ (the ratio of f_a to f_b), $\mathbf{M}_c$ (the moment magnitude of the critical earthquake), and $\Delta\sigma$ (the stress parameter). The values we chose for these and the other parameters in our model are given in Table 3. For λ we used Joyner's (1984) suggested value of 4. Joyner (1984) argued that the critical earthquake should be a moment magnitude 6.5 along the San Andreas fault system. In view of the possible cooler lithosphere and consequently greater seismogenic thickness in intraplate regions, we assigned the critical magnitude as $\mathbf{M}_c = 7.5$, realizing that this number is very uncertain.

The other parameters are those used by Boore and Atkinson (1987) and Atkinson and Boore (1990). Of these parameters, $\Delta\sigma$ is the most important. Based on scanty data, Boore and Atkinson (1987) chose 100 bars. Subsequent determinations of spectral amplitudes for intraplate earthquakes throughout the world by Boatwright and Choy (1987; J. Boatwright, written comm., 1990) suggest values averaging around 20 to 30 bars. (On account of directivity, values of $\Delta\sigma$ determined by Boatwright and Choy from teleseismic data may need to be increased by as much as a factor of 2 for use in the ground-motion simulations by point-source models (Boore and Joyner, 1989).) The recent Saguenay, Quebec, earthquake, on the other hand, had a stress parameter in excess of 200 bars (Fig. 12 in Boore and Atkinson, 1989). Furthermore, a study of seismic intensities by Hanks and Johnston (1992) suggests that stress parameters for earthquakes in eastern North America are larger than for western North America. Results in Boore (1986) and in a recently completed study by

TABLE 3

PARAMETERS OF THE STOCHASTIC MODEL

Source Properties	
$\rho_0 = 2.70$ gm/cm^3	$\beta_0 = 3.50$ km/sec
$\mathbf{M}_c = 7.5$	$\lambda = 4$
$\Delta\sigma = 100$ bars	
Path Properties	
$Q = 1100 f^{0.17}$	
$1/r$ geometrical spreading	
Duration $= 1/f_a + 0.05r$	
Site Properties	
Partition factor = 0.71	Radiation coefficient = 0.55
$\kappa_0 = 0.02$ sec	Free surface factor = 2.0
Amplification factor: equation (3), Table 2	

Boore and Joyner (1992) suggest that a stress parameter near 70 bars with a κ_0 close to 0.02 explains the strong-motion data from western North America. If Hanks and Johnston are correct, then the results of the western North America studies imply that, on the average, $\Delta\sigma$ should be larger than 70 bars for earthquakes in eastern North America. In view of these tenuous arguments, and lacking compelling evidence to the contrary, we decided to keep the stress parameter at 100 bars.

Attenuation Equations

We simulated ground motions for 17 distances ranging in equal logarithmic steps from 10 to 400 km and for moment magnitudes from 5.0 to 8.5, in steps of 0.25 magnitude units. The ground motions included peak acceleration (a_{max}) and 5%-damped, pseudorelative velocity response spectra (S_V) for 13 periods (12 of which were used by Joyner and Boore (1982, 1988). For each ground-motion parameter, the 255 simulated motions were fit to a simple function of magnitude and distance. To provide for a convenient form for use in generating seismic-hazard maps, the functional forms were kept as simple as possible. As we will subsequently see, this entailed some compromises in fitting the simulated data.

Following Joyner and Boore (1981), a two-step regression was used to fit the equations to the simulated data. The first step was to find the distance attenuation, given by the following equation:

$$\log y = E_i - \log r + kr, \tag{7}$$

where y is the ground-motion parameter, E_i is an offset factor for each earthquake, k is an attenuation factor (always negative), and r is the hypocentral distance in km (the calculations assume a point source). This equation assumes that the shape of the attenuation is the same for all magnitudes. The simulated data show this to be a poor assumption for higher-frequency motions for the broad range of distances represented by the simulated data (this is shown in a later figure). Rather than complicate the functional form to account for this (as Boore and Atkinson, 1987, did), we used an iterative, subjective procedure, guided by the notion that mismatches could be tolerated at large distances for small earthquakes but not for large earthquakes (the ground motions from small earthquakes at large distances are too small to cause any significant damage).

The first step in each iteration was to choose a value for k (guided by an initial regression determination with k in equation (7) as a free variable) and use regression to find the offset factors E_i. The second step used the offset factors to determine the magnitude scaling. Because we wanted prediction equations in terms of moment magnitude (**M**) and Nuttli magnitude (m_N, also known as m_{Lg} or m_{bLg}), we performed two separate regressions. In the first we fit a polynomial in **M** to E_i, and in the second we first converted **M** to m_N by inverting the equation of Atkinson and Boore (1987)

$$\mathbf{M} = 2.689 - 0.252 m_N + 0.127 m_N^2 \tag{8}$$

before doing the second regression. In our initial analyses, we used a single quadratic equation for the second regression. Because of the change in scaling at the critical-sized earthquake, however, we found that the fit to the offset

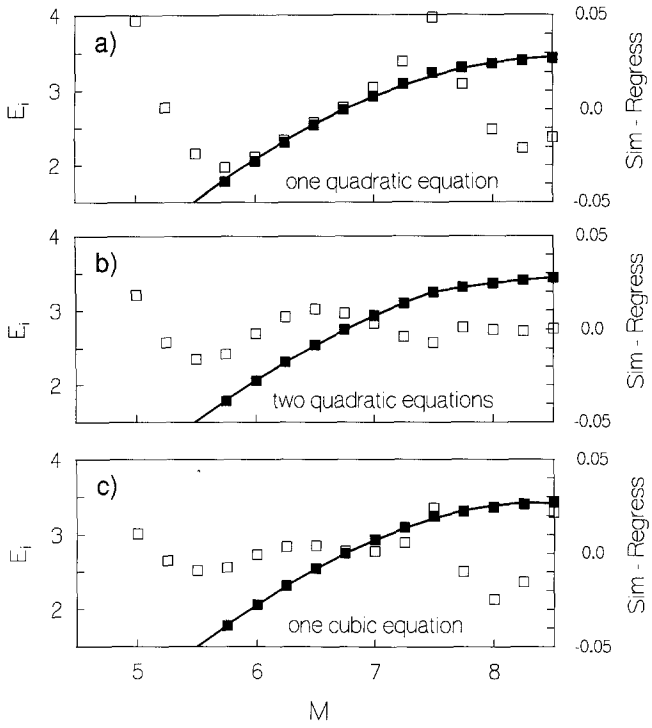

FIG. 4. Offset factors (filled squares, left ordinate) and difference between the simulated and computed offset factors (squares, right ordinate) as a function of moment magnitude. The factors are for 5%-damped response spectra at a period of 4 sec. The regression fit to the offset factors is given by the solid line. The offset factors were fit with (a) a single quadratic in magnitude, (b) two quadratics, on either side of $\mathbf{M} = 7.5$, and (c) a single cubic equation.

factors E_i was relatively poor. A sample of the fit to the E_i and the residuals of the fit for one of the worst cases is shown in Figure 4a . A much better fit was obtained by using two quadratic equations, one for earthquakes less than or equal to the critical earthquake ($\mathbf{M} = 7.5$) and one for larger earthquakes. Figure 4b shows the residuals for this fit. Twice as many coefficients are needed to describe this fit to the simulated data, however, and therefore we finally settled on a single cubic equation. The residuals, shown in Figure 4c, are tolerable. The cubic equation for the magnitude scaling is

$$E_i = a + b(m - 6) + c(m - 6)^2 + d(m - 6)^3, \tag{9}$$

where m is either $\mathbf{M}$ or m_N. The fit of this equation to the E_i factors are shown in Figure 5 for oscillator periods spanning the range considered in this paper. The residuals are generally less than 0.03 log units. Note also the change of magnitude scaling with oscillator period: short-period oscillators are much less sensitive to moment magnitude than are long-period oscillators. This conclusion is a straightforward and robust consequence of all source-spectral models and has been confirmed in a number of observational studies, including Joyner and Boore's (1982) analysis of strong-motion data from western North America.

After the two regressions were performed, the residuals between the simulated motions and those predicted from equations (7) and (9) were plotted. Plots of the residuals were produced for a series of attenuation coefficients k, and the

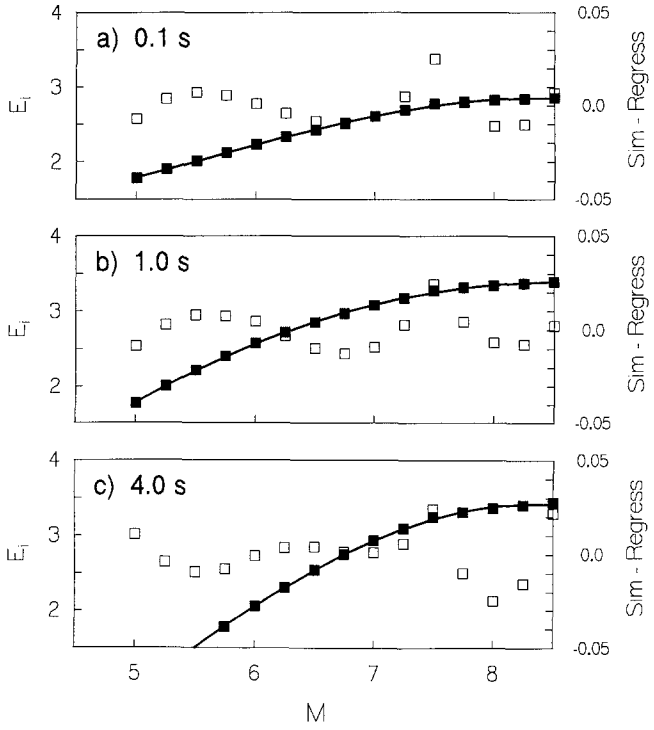

FIG. 5. As in Figure 4, but the three parts show the offset factors for the cubic equation and response spectra at periods of 0.1, 1.0, and 4.0 sec.

final value of k was chosen subjectively to reduce the residuals for large earthquakes at large distances, at the expense of the small-earthquake residuals (which are unimportant at large distances). As a final step, we sometimes found that adding a small scalar quantity a' to a in equation (9) also improved the overall fit. Weighted regression would have accomplished the same thing. The final prediction equation is given by combining equations (7) and (9):

$$\log y = a'' + b(m - 6) + c(m - 6)^2 + d(m - 6)^3 - \log r + kr, \qquad (10)$$

where $a'' = a + a'$. The coefficients for this equation are given in Tables 4 and 5. These tables are the primary contribution of this paper.

Note that a consequence of the cubic scaling with magnitude is that the predicted motion can actually decrease for large magnitudes. Such a decrease is, of course, not realistic and is an artifact of the particular functional form we chose for the magnitude scaling. The last column in Tables 4 and 5 gives the magnitudes beyond which the motions decrease. These magnitudes are large, and for practical purposes the equations can be used without regard to the possibility of decreases in motion. If for some reason motions are needed for magnitudes more than several tenths larger than the magnitudes in the last column, we recommend that the motions be equated to those for the magnitudes in the last column of the tables.

To see how well equation (10) matches the simulated data, we show in Figure 6 the difference between the simulated motions and those predicted from equation (10) as a function of distance. With the exception of magnitudes near

TABLE 4

COEFFICIENTS FOR GROUND-MOTION ESTIMATION AT DEEP-SOIL SITES IN EASTERN NORTH AMERICA IN TERMS OF **M***

T (sec)	a'	a''	b	c	d	k	**M** at max†
S_V							
0.05	0.020	1.946	0.431	−0.028	−0.018	−0.00350	8.35
0.10	0.040	2.267	0.429	−0.026	−0.018	−0.00240	8.38
0.15	0.015	2.377	0.437	−0.031	−0.017	−0.00190	8.38
0.20	0.015	2.461	0.447	−0.037	−0.016	−0.00168	8.38
0.30	0.010	2.543	0.472	−0.051	−0.012	−0.00140	8.47
0.40	0.015	2.575	0.499	−0.066	−0.009	−0.00110	8.50
0.50	0.010	2.588	0.526	−0.080	−0.007	−0.00095	8.48
0.75	0.000	2.586	0.592	−0.111	−0.001	−0.00072	8.58
1.00	0.000	2.567	0.655	−0.135	0.002	−0.00058	8.57
1.50	0.000	2.511	0.763	−0.165	0.004	−0.00050	8.55
2.00	0.000	2.432	0.851	−0.180	0.002	−0.00039	8.47
3.00	0.000	2.258	0.973	−0.176	−0.008	−0.00027	8.38
4.00	0.000	2.059	1.039	−0.145	−0.022	−0.00020	8.34
a_{max}	0.030	3.663	0.448	−0.037	−0.016	−0.00220	8.38
S_{Vmax}	0.020	2.596	0.608	−0.038	−0.022	−0.00055	8.51
S_{Amax}	0.040	4.042	0.433	−0.029	−0.017	−0.00180	8.40

*The distance used in equation (10) is generally the hypocentral distance; we suggest (based on unpublished work in progress) that, close to long faults, the distance should be the nearest distance to seismogenic rupture. The response spectra are for random horizontal components and 5% damping. The units of a_{max} and S_A are cm/sec^2; the units of S_V are cm/sec. The coefficients in this table should not be used outside the ranges $10 \leqq r \leqq 400$ km and $5.0 \leqq \mathbf{M} \leqq 8.5$.

†"**M** at max" is the magnitude at which the cubic equation attains its maximum value; for larger magnitudes, we recommend that the motions be equated to those for "**M** at max."

5, the residuals are very small for the longer-period oscillators. For the shorter-period oscillators, however, the residuals are larger and show systematic variations with distance. The variations are the result of trying to account for magnitude-dependent attenuation with the simple functional relation in equation (7). As mentioned earlier, we sought to keep the residuals for the small and large earthquakes within reasonable limits at small and large distances, respectively, by choosing k and a'' appropriately. As is clear from Figure 6c, this results in some compromises.

As a convenient summary of our predicted motions, Figure 7 shows our predicted pseudoacceleration spectra at periods of 0.3 and 1.0 sec as a function of distance for a suite of magnitudes, and in Figure 8 we compare our predictions for a generic deep soil site with the rock-site predictions of Atkinson and Boore (1990) as a function of oscillator period for several distances and magnitudes. Over most of the period range shown, the soil motions are uniformly above the rock motions by factors of 1.4 to 2.0. This is larger than the difference between code site coefficients for soil and rock. The differences between soil and rock shown in Figure 8, however, are similar to those indicated by data in the western United States for periods greater than about 0.5 sec (Joyner and Boore, 1988).

CONSTRUCTION OF RESPONSE SPECTRA FOR BUILDING CODES: A PROPOSAL

The modern approach to developing seismic design requirements for buildings dates back to ATC-3 (Applied Technology Council, 1978), whose provisions are

TABLE 5

COEFFICIENTS FOR GROUND-MOTION ESTIMATION AT DEEP-SOIL SITES IN EASTERN NORTH AMERICA IN TERMS OF m_N*

T (sec)	a'	a''	b	c	d	k	m_N at max†
S_V							
0.05	0.020	1.835	0.575	0.043	−0.075	−0.00350	7.80
0.10	0.040	2.156	0.571	0.045	−0.074	−0.00240	7.82
0.15	0.015	2.264	0.583	0.036	−0.071	−0.00190	7.83
0.20	0.015	2.345	0.600	0.025	−0.068	−0.00168	7.84
0.30	0.010	2.421	0.640	−0.001	−0.061	−0.00140	7.86
0.40	0.015	2.446	0.682	−0.026	−0.055	−0.00110	7.88
0.50	0.010	2.452	0.724	−0.050	−0.050	−0.00095	7.89
0.75	0.000	2.431	0.827	−0.100	−0.041	−0.00072	7.90
1.00	0.000	2.395	0.920	−0.133	−0.039	−0.00058	7.89
1.50	0.000	2.310	1.077	−0.169	−0.044	−0.00050	7.85
2.00	0.000	2.207	1.199	−0.174	−0.056	−0.00039	7.83
3.00	0.000	2.000	1.356	−0.129	−0.094	−0.00027	7.78
4.00	0.000	1.784	1.425	−0.044	−0.135	−0.00020	7.77
a_{max}	0.030	3.547	0.602	0.028	−0.071	−0.00220	7.82
S_{Vmax}	0.020	2.439	0.808	0.057	−0.093	−0.00055	7.92
S_{Amax}	0.040	3.930	0.578	0.039	−0.072	−0.00180	7.83

* The distance used in equation (10) is generally the hypocentral distance; we suggest (based on unpublished work in progress) that, close to long faults, the distance should be the nearest distance to seismogenic rupture. The response spectra are for random horizontal components and 5% damping. The units of a_{max} and S_A are cm/sec^2; the units of S_V are cm/sec. The coefficients in this table should not be used outside the ranges $10 \leqq r \leqq 400$ km and $5.4 \leqq m_N \leqq 7.8$.

† "m_N at max" is the magnitude at which the cubic equation attains its maximum value; for larger magnitudes we recommend that the motions be equated to those for "m_N at max."

based on approximate response spectra. These approximate spectra are proportional to "effective peak acceleration" at short periods and to "effective peak velocity" at long periods. ATC-3 provides maps intended to show effective peak acceleration and effective peak velocity corresponding to a 10% probability of exceedence in a 50-yr period. The use of two parameters for scaling the design response spectrum (as proposed by Newmark and Hall, 1982) is preferable to scaling by peak acceleration alone, because use of two parameters permits partial accommodation for the significant variation in shape of response spectra with changing earthquake magnitude and site conditions. The ATC approach was incorporated in the NEHRP Recommended Provisions for the Development of Seismic Regulations for New Buildings (Building Seismic Safety Council, 1985, 1988).

More recently, the concept has been introduced of using response values themselves at two or more periods as scaling parameters in developing approximate spectra for use in seismic design requirements. The Building Seismic Safety Council's Technical Subcommittee No. 1 (Algermissen *et al.*, 1991) has proposed the use of the 5%-damped pseudoacceleration response at 0.3 sec ($S_A(0.3)$) and 5%-damped pseudovelocity response at 1.0 sec ($S_V(1.0)$). The concept is based on the assumptions, true in western North America, that the pseudoacceleration response tends to be approximately constant for periods around 0.3 sec, and the pseudovelocity response tends to be approximately constant for periods around 1.0 sec. Since the pseudoacceleration response is

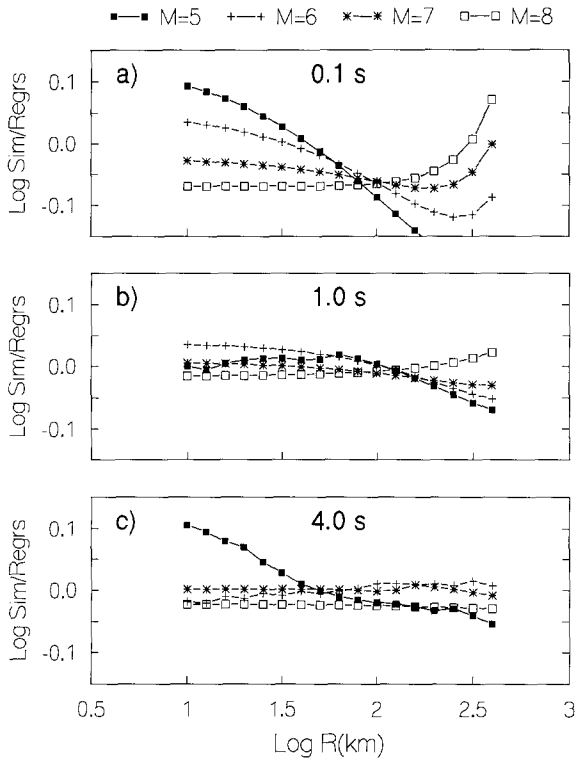

FIG. 6. The difference between the simulated data and the estimations from equation (10) for response spectra at periods of 0.1, 1.0, and 4.0 sec, as a function of distance for a suite of moment magnitudes.

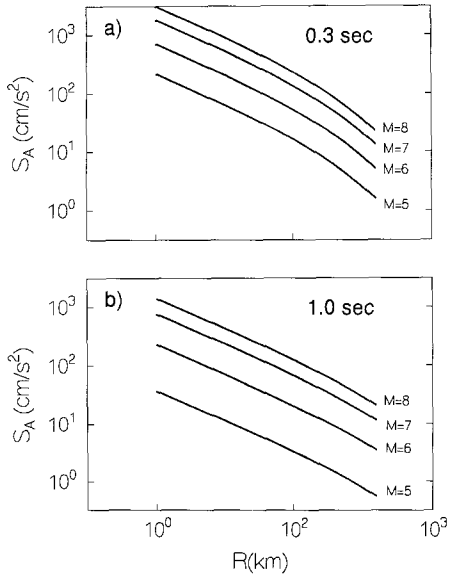

FIG. 7. Attenuation curves predicted from the results in this paper for pseudoacceleration spectra at periods of 0.3 and 1.0 sec.

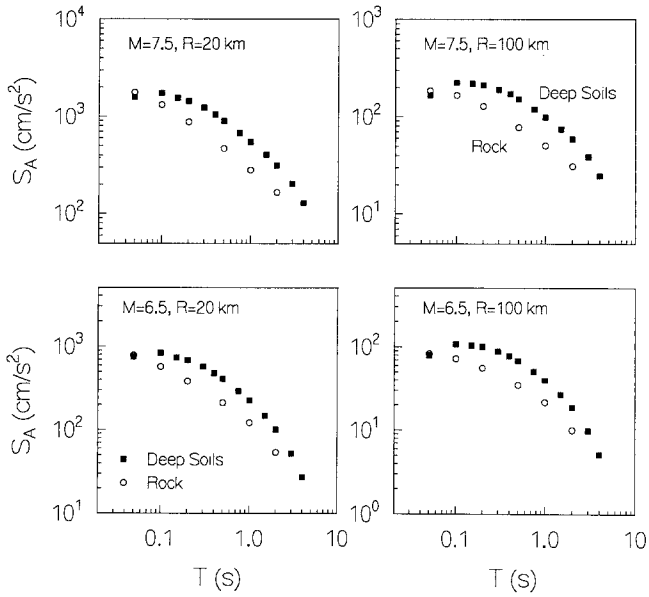

FIG. 8. Comparison of pseudoacceleration spectra in central and eastern North America at hard-rock and deep-soil sites, both based on the same methodology. The comparison is for moment magnitudes of 6.5 and 7.5 and hypocentral distances of 20 and 100 km. The soil motions are from this paper, and the rock motions are from Atkinson and Boore (1990).

equal to $2\pi/T$ times the pseudovelocity response, the pseudoacceleration spectrum can be approximated in terms of S_A and S_V as

$$S_A \approx \begin{cases} S_A(0.3), & \text{for } T \leqq 2\pi S_V(1.0)/S_A(0.3) \\ 2\pi S_V(1.0)/T, & \text{for } T > 2\pi S_V(1.0)/S_A(0.3) \end{cases}. \tag{11}$$

When this concept was tried out at selected sites in the western United States with probabilistic calculations by E. V. Leyendecker using the attenuation equations of Joyner and Boore (1982, 1988), the approximate spectra computed using the two parameters $S_A(0.3)$ and $S_V(1.0)$ agreed well enough with spectra computed for the 12 periods used by Joyner and Boore. In eastern North America, however, the S_A for periods less than 0.3 sec are greater than $S_A(0.3)$ for most of the relevant magnitudes and distances if the equations given in this paper are used. The larger spectral values for periods less than 0.3 sec are a consequence of the lower values of κ_0 adopted for eastern North America (or equivalently, a higher f_{max}), corresponding to less attenuation at the site. How the large values at short periods affect the seismic design requirements is a question that we, as seismologists, will not and should not address. We are moved, however, to suggest a simple alternative that will ensure that the approximate spectrum will envelope the spectrum calculated at all periods of engineering interest. We define S_{Amax} and S_{Vmax} as the largest values of pseudoacceleration and pseudovelocity response, respectively, for 5% damping in the period range of engineering interest, taken here as 0.1 to 4 sec. The period range is an essential part of the definition. In eastern North America, higher values of pseudoacceleration may occur for periods less than 0.1 sec. We chose 0.1 to 4 sec to illustrate the concept; the final choice is a matter for

engineering judgement. S_{Amax} and S_{Vmax} are functions of magnitude and distance. Using these new quantities, the equations

$$S_A \approx \begin{cases} S_{Amax}, & \text{for } T \leqq 2\pi S_{Vmax}/S_{Amax} \\ 2\pi S_{Vmax}/T, & \text{for } T > 2\pi S_{Vmax}/S_{Amax} \end{cases} \quad (12)$$

will define the desired approximate spectrum.

An illustration of the two ways (equations 11 and 12) for estimating response spectra is given in Figure 9. The left panel shows the simulated spectrum at 32 km from a magnitude 7 earthquake, using the deep-soil model of this paper. The dashed lines show the approximate spectrum from equation (11), using S_A at 0.3 sec. The largest value of S_A occurs at a period of 0.1 sec, however, and therefore equation (11) leads to an underestimate of the spectrum for this magnitude and distance. The proposed method for approximating the spectrum (equation 12) produces an envelope of the simulated spectrum. The right panel of Figure 9 shows the comparison of the simulated and approximate spectra for a distance of 320 km. In this case, the largest value of S_A occurs at a period of 0.3 sec, and both approximate spectra are the same for short periods. The largest S_V of the simulated spectrum, however, occurs at 2.0 sec, and therefore the approximate spectrum based on fixed periods (equation 11) underestimates the simulated spectrum at long periods.

Tables 4 and 5 contain coefficients for S_{Vmax} and S_{Amax}. These quantities were determined by searching over the period range 0.1 to 4.0 sec for the maximum of the pseudovelocity and pseudoacceleration response spectrum for each pair of magnitudes and distances in the simulated data, and then fitting equation (10) to these derived data using the two-stage regression method. For completeness we include Table 6 , based on the attenuation equations of Joyner and Boore (1982, 1988), which can be used with equation (10) for computing S_{Amax} and S_{Vmax} at soil sites in western North America.

We should emphasize that determinations of S_{Amax} and S_{Vmax} should not be made using peak values of pseudoacceleration and pseudovelocity from individual observed records, for they will be biased toward high values and thereby not be usable for approximating probabilistic spectra. The appropriate procedure is first to derive equations giving the median values of pseudoacceleration as a

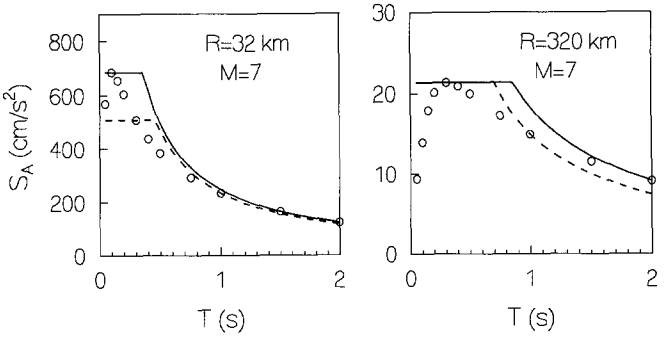

FIG. 9. Comparison of simulated pseudoacceleration spectra (circles) and approximations based on S_A and S_V at fixed periods of 0.3 and 1.0 sec (dashed line: equation 11) and on the largest values of S_A and S_V over the period range 0.1 to 4 sec (solid line: equation 12).

TABLE 6

COEFFICIENTS FOR S_{Vmax} AND S_{Amax} AT SOIL SITES IN WESTERN NORTH AMERICA IN TERMS OF **M***

	a''	b	c	d	k	$h^\dagger$
S_{Vmax}	2.528	0.673	−0.075	−0.041	−0.00196	5
S_{Amax}	3.931	0.329	−0.065	0.000	−0.00590	8

*The response spectra are for random horizontal components and 5% damping. The units of S_{Vmax} and S_{Amax} are cm/sec and cm/sec^2, respectively. The coefficients in this table can be used for $r_0 \leqq 100$ km and $5.0 \leqq \mathbf{M} \leqq 7.75$.

†The distance r used in equation (10) is obtained from $r = \sqrt{r_0^2 + h^2}$, where r_0 is the horizontal distance, in kilometers, to the nearest part of the vertical projection of the rupture surface to the earth's surface.

function of distance and magnitude for a suite of periods, and then use these to determine S_{Amax} and S_{Vmax}.

SUMMARY AND CONCLUSIONS

A generic model of shear velocity and attenuation for deep soil sites has been constructed from compilations by Bernreuter *et al.* (1985) and work by Andrews and Mooney (1985) and by Andrews (written comm., 1990), among others. We derived a filter accounting for the soil column by using the approximate method for computing the amplification and attenuation proposed by Joyner *et al.* (1981). This filter was combined with the stochastic model of Boore and Atkinson (1987) to generate equations for the estimation of response spectra, peak acceleration, and the maximum pseudovelocity and pseudoacceleration responses as a function of distance and magnitude. The equations are intended to give estimates of the median value of the motions for deep soil sites (class S2 in the Uniform Building Code) and are to be used in central and eastern North America, for moment magnitudes ranging from 5 to 8.5 and distances from 10 to 400 km. Equations are given both for moment magnitude (**M**) and for the short-period Nuttli magnitude (m_N). Direct comparison shows that the approximate method for computing the soil response is in good agreement with the response computed from exact calculations, even when a large step in seismic impedance exists at the bottom of the soil column. The maximum pseudovelocity and pseudoacceleration responses are introduced for the first time here, and a discussion is included of their possible use in determining the seismic coefficient in building codes.

ACKNOWLEDGMENTS

We thank J. C. Chen for providing the data used to construct Figure 1, Walt Silva for providing a convenient form of the average curve in Figure 1, Charles Mueller for his program that computes the exact *SH* response of soil columns, and E. V. Leyendecker and Ted Algermissen for discussion related to the use of the results in this paper. We thank Ken Campbell, C. B. Crouse, E. V. Leyendecker, and Erdal Şafak for their thoughtful reviews of the paper. This work was partially funded by a grant from the U.S. Nuclear Regulatory Commission.

REFERENCES

Algermissen, S. T., E. V. Leyendecker, G. A. Bollinger, N. C. Donovan, J. E. Ebel, W. B. Joyner, R. W. Luft, and J. P. Singh (1991). Probabilistic ground-motion hazard maps of response spectral ordinates for the United States, in *Proc. 4th Int. Conf. Seismic Zonation*, Stanford, California **II**, 687–694.

Andrews, M. and W. Mooney (1985). The relocation of microearthquakes in the northern Mississippi embayment, *J. Geophys. Res.* **90,** 10,223-10,236.

Applied Technology Council (1978). Tentative Provisions for the Development of Seismic Regulations for Buildings, Applied Technology Council Publication ATC 3-06, 505 pp.

Atkinson, G. M. and D. M. Boore (1987). On the m_N, **M** relation for eastern North America, *Seism. Res. Lett.* **58,** 119-124.

Atkinson, G. M. and D. M. Boore (1990). Recent trends in ground motion and spectral response relations for North America, *Earthquake Spectra* **6,** 15-35.

Bernreuter, D. L., J. B. Savy, R. W. Mensing, and J. C. Chen (1985). Seismic hazard characterization of 69 nuclear plant sites east of the Rocky Mountains, U.S. Nuclear Regulatory Commission NUREG/CR-5250, UCID-21517, Vol. 7.

Boatwright, J. and G. L. Choy (1987). Acceleration source spectra for large earthquakes in northeastern North America (abstract), *EOS* **68,** 1348.

Boore, D. M. (1986). Short-period *P*- and *S*-wave radiation from large earthquakes: implications for spectral scaling relations, *Bull. Seism. Soc. Am.* **76,** 43-64.

Boore, D. M. and G. M. Atkinson (1987). Stochastic prediction of ground motion and spectral response parameters at hard-rock sites in eastern North America, *Bull. Seism. Soc. Am.* **77,** 440-467.

Boore, D. M. and G. M. Atkinson (1989). Spectral scaling of the 1985 to 1988 Nahanni, Northwest Territories, earthquakes, *Bull. Seism. Soc. Am.* **79,** 1736-1761.

Boore, D. M. and W. B. Joyner (1989). The effect of directivity on the stress parameter determined from ground motion observations, *Bull. Seism. Soc. Am.* **79,** 1984-1988.

Boore, D. M., W. B. Joyner, and L. Wennerberg (1992). Fitting the stochastic ω^{-2} source model to observed response spectra in western North America: Tradeoffs between $\Delta\sigma$ and κ, *Bull. Seism. Soc. Am.* (submitted).

Building Seismic Safety Council (1985). *NEHRP Recommended Provisions for the Development of Seismic Regulations for New Buildings*, Building Seismic Safety Council, 3 parts, 471 pp.

Building Seismic Safety Council (1988). *NEHRP Recommended Provisions for the Development of Seismic Regulations for New Buildings*, Building Seismic Safety Council, 2 parts, 440 pp.

Hanks, T. C. and A. C. Johnston (1992). Some common features in the excitation and propagation of strong ground motion for North American earthquakes, *Bull. Seism. Soc. Am.* **82,** (in press).

Hanks, T. C. and R. K. McGuire (1981). The character of high-frequency strong ground motion, *Bull. Seism. Soc. Am.* **71,** 2071-2095.

Haskell, N. (1960). Crustal reflection of plane *SH* waves, *J. Geophys. Res.* **65,** 4147-4150.

Joyner, W. B. (1984). A scaling law for the spectra of large earthquakes, *Bull. Seism. Soc. Am.* **74,** 1167-1188.

Joyner, W. B. and D. M. Boore (1981). Peak horizontal acceleration and velocity from strong-motion records including records from the 1979 Imperial Valley, California, earthquake, *Bull. Seism. Soc. Am.* **71,** 2011-2038.

Joyner, W. B. and D. M. Boore (1982). *Prediction of earthquake response spectra, U.S. Geol. Surv. Open-File Rept. 82-977*, 16 pp.

Joyner, W. B. and D. M. Boore (1988). Measurement, characterization, and prediction of strong ground motion, in *Proc. Earthquake Eng. Soil Dyn. II*, GT Div/ASCE, Park City, Utah, 27-30 June, 1988, 43-102.

Joyner, W. B., R. E. Warrick, and T. E. Fumal (1981). The effect of Quaternary alluvium on strong ground motion in the Coyote Lake, California, earthquake of 1979, *Bull. Seism. Soc. Am.* **71,** 1333-1349.

Newmark, N. M. and W. J. Hall (1982). *Earthquake Spectra and Design*, Earthquake Engineering Research Institute, El Cerrito, CA, 103 pp.

Uniform Building Code (1988). *Uniform Building Code*, International Conference of Building Officials, Whittier, CA, 926 pp.

APPENDIX:
CHECKING THE VALIDITY OF THE METHOD FOR ESTIMATING SOIL RESPONSE

Several studies have compared the soil response computed from the simplified method proposed by Joyner *et al.* (1981) with the response from a complete solution that accounts for the reverberations and the leakage of energy into the half-space beneath the soil column. J. Boatwright (personal comm., 1987) and W. Silva and R. Darragh (personal comm., 1987) have made such tests, and

they find reasonable agreement between the estimates of the site response from the two methods. These earlier tests have demonstrated the general reliability of the simplified method. We report on some similar studies in this appendix. It is not our aim to do a comprehensive analysis. Rather, we were curious about the comparison of the simplified and exact site responses for the soil model used in our study (Table 1 and Fig. 2). The velocity profile in the soil model has a large contrast in shear velocity at the base of the sediments, and this contrast will produce reverberations not accounted for in simplified analyses of site response. As in the earlier studies, we compared the site response computed using both the simplified method described earlier and the wave-theory calculation due to Haskell (1960). We consider only vertically propagating *SH* waves, using the program RATTLE from C. Mueller. The κ_0 factor to be used in the diminution factor (equation 2) was computed by summing $z/(\beta Q)$ over the entire thickness of sediments; the result was $\kappa_0 = 0.03$. The velocity, density, and Q distributions used in the wave-theory calculations are those tabulated in Table 1.

The impulse response at the surface (Fig. A1) shows that the direct wave dominates the motion. Because the simplified method does not account for reverberations, we thought it would be instructive to compute spectra for a series of windows of increasing length. Accordingly, we computed the spectra from the time series in Figure A1 for windows that include the direct wave and zero, one, two, and more than 10 reverberations. The results are shown in Figure A2 as a series of curves. The spectra were normalized to the value that would be obtained at the surface of a half-space made up of the rock under the sediments. In spite of the apparent dominance of the direct arrival in the time domain (Fig. A1), the transfer function is highly dependent on the reverberations. Although interesting, this observation is a side issue. The point of this appendix is to compare the exact response (lines in Fig. A2) with that computed from the simplified method (solid circles in Fig. A2). At higher frequencies, the simple method overestimates the response of the direct wave but gives a smoothed approximation of the complete response, including all reverberations. The differences in response-spectral values computed using the simple and exact soil-effect calculations would be less than the differences in Fourier spectra

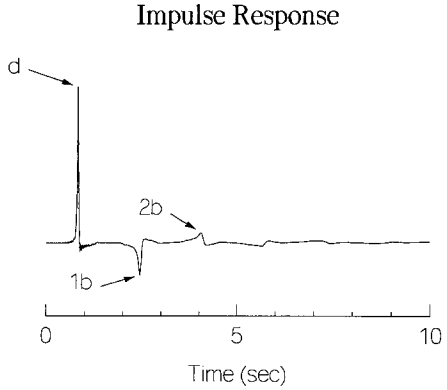

FIG. A1. The impulse response for vertically propagating *SH* waves in the soil column of Figure 2. The arrows indicate the direct arrival (d) and the arrivals that have made an additional one and two round trips through the entire soil column (1b and 2b, respectively).

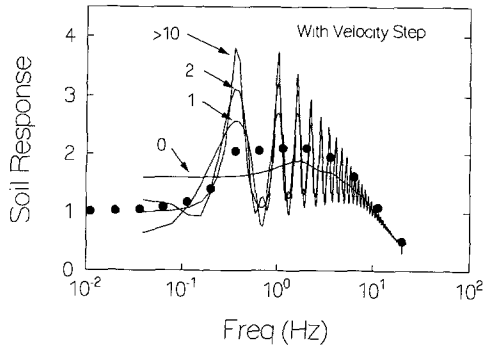

FIG. A2. The soil response, relative to a half-space without the soil column. The solid circles are the response predicted by the approximate method of Joyner *et al.* (1981); the curves are the response from the exact calculations. Different numbers of reverberations, indicated by the labels, are included in the exact response.

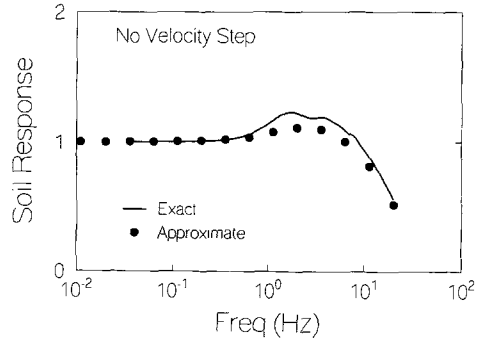

FIG. A3. As in Figure A2, but for a model without a step at the bottom of the soil column. In this case there are no reverberations, and the spectrum from only one exact calculation is shown. Note the scale change on the ordinate between this and the previous figure.

shown in Figure A2. In the worst case, the errors produced in the response spectral estimations by using the simple correction for the soil response would be comparable to the errors in ground-motion prediction based on the empirical analysis of data.

We also computed the response of the soils without a step increase at the bottom (in other words, we let layer 29 in the model shown in Table 1 be the half-space). As expected, the amplification is smaller than when the soil column is terminated by a high-velocity halfspace (Fig. A3). In this case, the response from the simple method underestimates the exact response, but only by about 25%.

We conclude that the soil response computed from the simple method proposed by Joyner *et al.* (1981) gives an adequate approximation of the site response, even for cases involving large step changes in impedance (for which reverberations in the soil column are important).

U.S. GEOLOGICAL SURVEY
MAIL STOP 977
345 MIDDLEFIELD ROAD
MENLO PARK, CALIFORNIA 94025

Manuscript received 25 January 1991